Coexistence of Metallocene Cations and Anions

Authors: Nico Gino Kub, Robin Sievers, Marc Reimann, Tim-Niclas Streit, Simon Steinhauer, Johanna Schlögl, Martin Kaupp, Moritz Malischewski*

Author affiliations:

N. G. Kub, R. Sievers, T.-N. Streit, S. Steinhauer, J. Schlögl, M. Malischewski: Freie Universität Berlin, Institut für Chemie und Biochemie – Anorganische Chemie, Fabeckstr. 34-36, 14195 Berlin, Germany.

M. Reimann, M. Kaupp: Technische Universität Berlin, Institut für Chemie, Straße des 17. Juni 135, 10623 Berlin, Germany

Abstract

We report the synthesis and structural characterization of the rhodocene anion $[Rh(C_5(CH_3)_5)(C_5(CF_3)_5)]^-$ [**1**]$^-$ as the $[Co(C_5(CH_3)_5)_2]^+$ salt, representing an unprecedented coexistence of metallocene cations and anions in different oxidation states. [**1**]$^-$ was synthesized by the reduction of the rhodocenium cation $[Rh(C_5(CH_3)_5)(C_5(CF_3)_5)][BF_4]$ [**1**]$^+$[BF_4]$^-$ with two equivalents of decamethylcobaltocene $[Co(C_5(CH_3)_5)_2]$, since the strongly electron-withdrawing effect of the $[C_5(CF_3)_5)]^-$ ligand shifts the first and second reduction potentials of [**1**]$^+$ to moderate values of −0.90 V and −1.46 V vs Fc^+/Fc. The respective salt $[Co(C_5(CH_3)_5)_2]^+$[**1**]$^-$ was characterized by single crystal X-ray diffraction (XRD), also providing the first example of an isolated and structurally characterized 4d metallocene anion. Whereas the Rh(III) cation has two η^{5-} bound Cp ligands, the perfluorinated Cp* ligand is only η^3-bound in the Rh(I) anion in order to obey the 18 electron rule. The reduction of the rhodocenium center is also accompanied by a significant shift of the ^{103}Rh NMR signal from −9308 ppm [**1**]$^+$ to −6895 ppm [**1**]$^-$ (referenced to $Rh(acac)_3$), reflecting the change in coordination geometry.

Introduction

The synthesis and characterization of ferrocene (Fc) in 1951 has been widely marked as the birth of organometallic chemistry, sparking the rich chemistry of metallocenes.[1] Besides many prosperous applications ranging from medicinal chemistry,[2] battery design,[3] atomic sensors[4] to catalysis[5], a defining feature of metallocenes is their unmatched redox chemistry, with the one electron oxidation of ferrocene to ferrocenium serving as standard reference for non-aqueous electrochemical processes.[6] Considering that transition metal metallocenes usually

traverse between formal +II and +III oxidation states, corresponding to the neutral metallocene [MCp_2] (M = metal, Cy = cyclopentadienyl) and cationic metallocenium [MCp_2]$^+$, the further expansion of these boundaries has gained a lot of attention in recent years.[7] The synthesis and characterization of the nickelocenium dication[8] and decamethylferrocene dication[9] mark recent advances in the oxidation of metallocenes to the formal +IV metal oxidation state.

Compared to the synthesis of metallocene cations, metallocene anions have remained far less explored with only a handful of synthetically isolated compounds.[10] As metallocene anions require a formal +I metal oxidation state, group 1 metallocenes represent the simplest metallocene anions. Since the +I oxidation state is most stable for alkali metals, the synthesis of group 1 metallocene anions is not dependent on any reducing agents or bulky Cp substituents.[10j-m] In contrast, the unstable nature of d-block metallocene anions not only demands harsh reducing agents for their synthesis, but also the stabilization of these highly reactive anionic species. Recent approaches, such as the isolation of the derivatized manganocene, ferrocene and cobaltocene anion,[10i] have demonstrated the efficiency of bulky substituents in stabilizing the reactive metal center.

As harsh reductive conditions are required to generate metallocene anions, inert spectator cations are a necessity. Thus far, alkali metal cations have been the sole choice, as their reduction potentials surpass those of the corresponding metallocene anions.[10a] In principle, other cations could also be suitable, given that their reduction potential transcends that of the corresponding metallocene anion. While this has never been realized, the substantial effect of Cp substitution patterns on the redox properties of metallocenes could principally allow metallocene cations and anions to coexist in one compound. As decamethylcobaltocenium [$Co(C_5(CH_3)_5)_2$]$^+$ has one of the lowest reduction potentials (E = −1.94 V, in CH_2Cl_2 vs Fc^+/Fc) of a metallocene cation, the corresponding metallocene anion must exceed this reduction potential sufficiently to prevent decomposition by electron transfer resulting in two neutral metallocenes.[11]

While not yet investigated in this context, the introduction of fluorinated electron withdrawing substituents into the Cp scaffold offers a novel approach towards isolating metallocene anions with dramatically increased redox potentials. This has been demonstrated exemplarily for ferrocenes, whereby the addition of every fluorine substituent increases the redox potential by $E_{1/2}$ = +0.14 V (in CH_2Cl_2 vs. Fc^+/Fc), with the oxidation of pentafluoroferrocene [$Fe(C_5H_5)(C_5F_5)$] occurring at $E_{1/2}$ = +0.82 V (in CH_2Cl_2 vs. Fc^+/Fc).[12] This effect is substantially more pronounced for trifluoromethyl groups (CF_3) due to the absence of conjugated donor effects, with two CF_3 substituents increasing the redox potential by a staggering $E_{1/2}$ = +0.64 V (in CH_2Cl_2 vs. Fc).[13] Additionally, CF_3 groups also offer a greater steric shielding compared to fluorine substituents.

The first synthesis of the perfluorinated Cp* was described in 1980 by Lemal *et. al.* and later improved by Chambers *et. al.*.[14] In previous works we have demonstrated the first coordination of $[C_5(CF_3)_5]^-$ and the unique reactivity towards substitution lability, as well as the increased oxidative stability compared to ordinary Cp ligands.[14-15] In preliminary works we have shown, that the incorporation of $[C_5(CF_3)_5]^-$ into ferrocene shifts the redox potential of $[Fe(C_5H_5)(C_5(CF_3)_5]$ by ≈1.4 V to more positive values.[16] Hereby, metallocenes bearing $[C_5(CF_3)_5]^-$ as a ligand could enable the synthesis of a metallocene anion with a redox potential significantly more positive than −2 V, thereby allowing the synthesis and isolation of a metallocene anion paired with decamethylcobaltocenium $[Co(C_5(CH_3)_5)_2]^+$ as a counter ion.[11a]

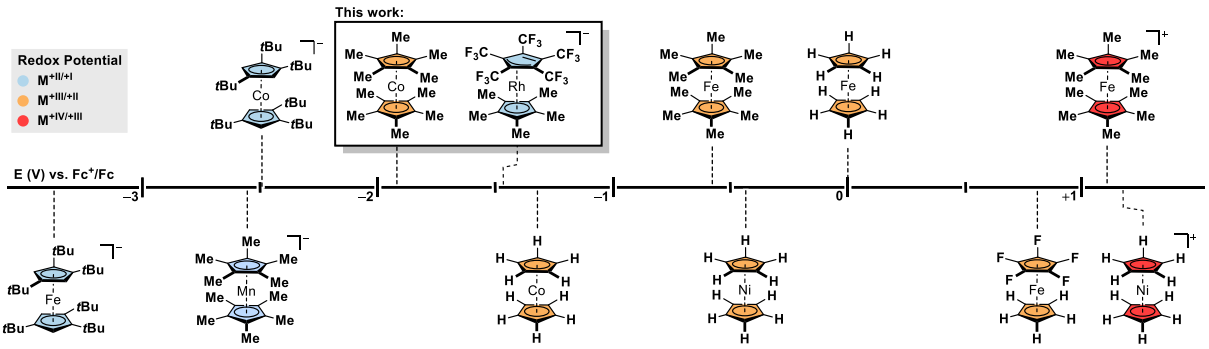

Figure 1. Experimentally obtained redox potentials in V versus Fc^+/Fc of various metallocene anions,[10c, 10i, 17] neutral metallocenes,[8, 11a, 12b] and metallocene cations.[8-9]

Results and Discussion

The synthesis of the mixed rhodocenium $[\mathbf{1}]^+[BF_4]^-$ was achieved by the reaction of $[Rh(C_5(CH_3)_5Cl_2]_2$ and $[Ag][BF_4]$ to achieve an in situ formation of the solvated 12 electron fragment $[Rh(C_5(CH_3)_5)]^{2+}$ in the presence of $[NEt_4][C_5(CF_3)_5]$. After purification $[\mathbf{1}]^+[BF_4]^-$ was isolated with an overall yield of 49% and represents the first rhodocenium species with $[C_5(CF_3)_5]^-$ as a ligand (Scheme 1). The ^{19}F NMR spectrum revealed a singlet at δ = −51.8 ppm (in CD_2Cl_2), which is high-field shifted compared to the ionic $[C_5(CF_3)_5]^-$ signal (δ = −50.5 ppm in CD_2Cl_2). The ^1H NMR revealed a singlet at δ = 2.14 ppm (in CD_2Cl_2) for the $[C_5(CH_3)_5]^-$ coligand. Additionally, a rhodium shift was observed in the ^1H, ^{103}Rh HMQC spectrum at δ = −9308 ppm (in CD_2Cl_2, Figure S5 in SI). Single crystals of $[\mathbf{1}]^+[BF_4]^-$ were obtained by slowly cooling a mixture of CH_2Cl_2 and *n*-pentane to −75 °C, crystallizing in the triclinic space group $P\bar{1}$. The asymmetric unit with two $[\mathbf{1}]^+[BF_4]^-$ moieties revealed a η^5-coordination of both the $[C_5(CF_3)_5]^-$ and $[C_5(CH_3)_5]^-$ ligands (Figure S11 in SI). Interestingly, the averaged $Rh-C_{Cp}$ bond length for $[C_5(CF_3)_5]^-$ (2.222(8) Å) is slightly larger compared to the averaged $Rh-C_{Cp}$ bond length for $[C_5(CH_3)_5]^-$ (2.174(9) Å), while the $C_{Cp}-C_{Cp}$ distances are relatively similar for both Cp ligands.

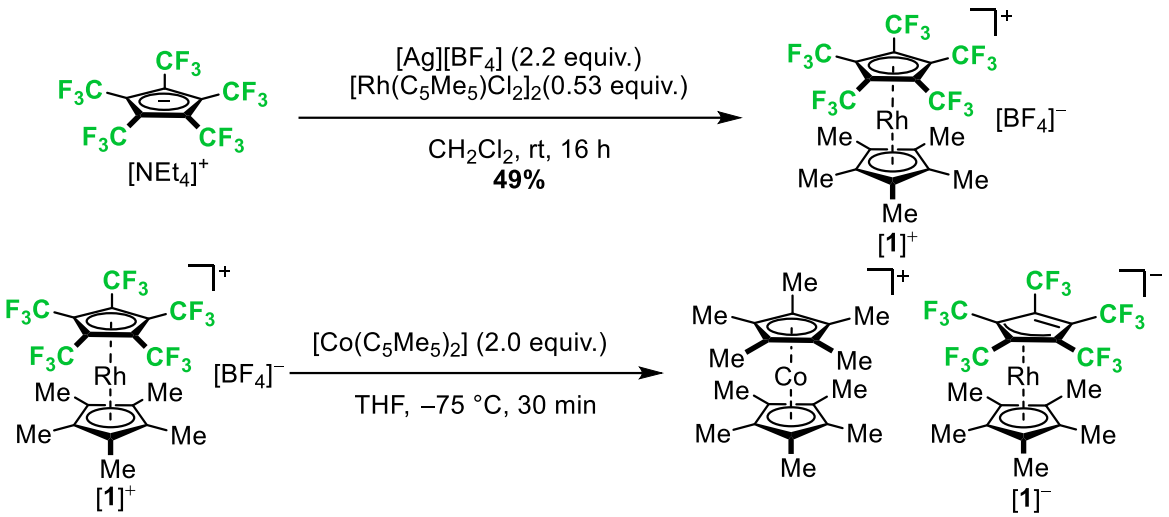

Scheme 1. Synthesis of $[Rh(C_5(CH_3)_5)(C_5(CF_3)_5)][BF_4]$ from $[NEt_4][C_5(CF_3)_5]$ and $[Rh(C_5(CH_3)_5)Cl_2]$ (top). Reduction of $[\mathbf{1}]^+[BF_4]^-$ with $[Co(C_5(CH_3)_5)_2]$ towards $[Co(C_5(CH_3)_5)_2]^+[\mathbf{1}]^-$ (bottom).

To determine the reduction potentials of the corresponding rhodocene [**1**] and rhodocene anion $[\mathbf{1}]^-$, a cyclic voltammogram was measured of a tetrahydrofuran (THF) solution of $[\mathbf{1}]^+[BF_4]^-$ at room temperature, with $[NBu_4][PF_6]$ as additional electrolyte (Figure 2). A quasi-reversible reduction process was observed at $E_{1/2}$ = −0.90 V (vs $Fc^{+/0}$) which likely corresponds to the Rh^{+III}/Rh^{+II} one electron reduction towards the neutral rhodocene. For further investigations $[\mathbf{1}]^+[BF_4]^-$ was reduced with $[Co(C_5H_5)_2]$ in THF at −20 °C, which lead to the immediate formation of a dark blue suspension. The neutral rhodocene [**1**] was investigated via EPR spectroscopy. The X-band spectrum at −196 °C revealed a single feature around g_{iso} = 1.968, suggesting a doublet spin state with a delocalized electron (Figure S14 in SI). Due to solubility issues and decomposition at temperatures above −20 °C, it was not possible to obtain single crystals of [**1**]. A second quasi-reversible reduction process was observed at $E_{1/2}$ = −1.46 V (vs $Fc^{+/0}$) and likely corresponds to the Rh^{+II}/Rh^{+I} one electron reduction towards the rhodocene anion. Compared to other substituted rhodocenium derivatives, $[\mathbf{1}]^+[BF_4]^-$ revealed substantial increases of redox potentials of up to 1.0 V for both the first and second reduction.[18] Similar to the introduction of an indenyl ligand $[C_9H_7]$, the $[C_5(CF_3)_5]^-$ ligand enhances the stability of the neutral and anionic rhodocene through increased redox potentials, resulting from a strong electron withdrawing effect, as well as a facilitated η^5/η^3-ring slippage, which results in a 18 electron rather than 20 electron complex.[18c] Based on the observed reduction potential towards the rhodocene anion and the relative position towards the oxidation potential of decamethylcobaltocene $[Co(C_5(CH_3)_5)_2]$, the latter was assumed to be a suitable reducing agent.

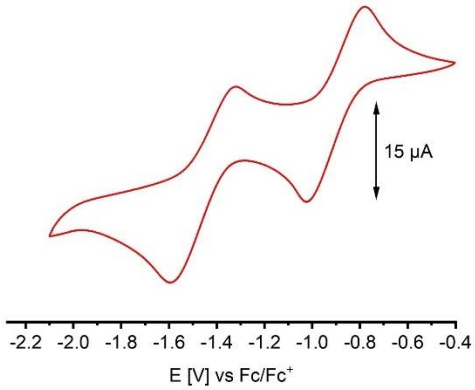

Figure 2. Cyclic voltammogram (current in µA versus potential in V versus Fc/Fc^+; Scan rate: 100 mV/s) of $[Rh(C_5(CH_3)_5)(C_5(CF_3)_5)][BF_4]$ (14 µmol) in anhydrous degassed THF with 0.1 M $[NBu_4][PF_6]$ as an electrolyte.

Consequently, the twofold reduction of $[\mathbf{1}]^+[BF_4]^-$ with $[Co(C_5(CH_3)_5]$ in THF at −75 °C was carried out, resulting in the formation of $[Co(C_5(CH_3)_5)_2]^+[\mathbf{1}]^-$, which marks the first instance of a stable metallocene cation and anion coexisting in one compound. As the reduction chemistry of rhodocene cations is notoriously challenging,[18b, 18c] the synthesized $[Co(C_5(CH_3)_5)_2]^+[\mathbf{1}]^-$ represents the first isolated and structurally characterized rhodocene anion, and also the first 4d metallocene anion to date.

The ^{19}F NMR spectrum revealed three singlet signals at δ = −49.3 ppm, −53.3 ppm and −58.1 ppm, indicating a η^3-coordination of $[C_5(CF_3)_5]^-$, where the individual positions seem to be locked, or the exchange is slower than the experiment. Slow decomposition was already observed starting at −70 °C, further supporting the temperature sensitivity of the rhodocene anion. Furthermore, a rhodium shift was observed in the ^1H, ^{103}Rh HMQC spectrum at δ = −6895 ppm (in THF-d^8, vs $Rh(acac)_3$, Figure S10), which is 2413 ppm more positive than the shift of the corresponding cationic Rh(III) compound (−9308 ppm). Quantum chemical calculations of the ^{103}Rh shifts at quasirelativistic two-component ZORA level (see Supporting Information) find excellent agreement for both species (−6610 ppm and −9570 ppm, respectively). Additional calculations of the Rh(III) species at the structure of the Rh(I) species find a shift of −7090 ppm, suggesting that the less negative shift results predominantly from the lower coordination number in the Rh(I) complex.

For further structural confirmation, single crystals of $[Co(C_5(CH_3)_5)_2]^+[\mathbf{1}]^-$ were obtained by layering a saturated THF solution with *n*-hexane at −75 °C. The respective salt crystallized in the monoclinic space group $P2_1/n$, with one $[Co(C_5(CH_3)_5)_2]^+[\mathbf{1}]^-$ fragment in the asymmetric unit (Figure 3, left). The $Co-C_{Cp}$ averaged bond length of 2.047(7) Å corresponds to published $Co-C_{Cp}$ bond lengths of other $[Co(C_5(CH_3)_5)_2]^+$ compounds and is significantly shorter than the $Co-C_{Cp}$ averaged bond length of 2.099(9) Å of $[Co(C_5(CH_3)_5)_2]$, confirming the cationic nature

of the cobaltocene species.[19] The η³-coordination of the $[C_5(CF_3)_5]^-$ ligand in $[\mathbf{1}]^-$ is most notable. It is perfectly reproduced in quantum chemical calculations at the r²SCAN-3c level (see SI). As the reduced π-donor ability of $[C_5(CF_3)_5]^-$ coincides with smaller M−Cp interaction energies,[13a] which facilitates a η⁵/η³ ring slippage, the η³-coordination effectively reduces the Pauli repulsion between the Rh(I) center and the $[C_5(CF_3)_5]^-$ ring originating from the population of antibonding orbitals upon reduction (see Table S3 in SI) and thereby stabilizes the anionic species. This also lowers the symmetry of the system, avoiding a low-spin 20 electron metallocene, resulting in a more stable 18 electron system. While the terminal positions (C2, C5) of the $[C_5(CF_3)_5]^-$ allylic binding motive exhibit an average Rh−C_{Cp} bond length of 2.198(7) Å, the central position (C1) has a significantly shortened Rh−C_{Cp} bond length of 2.007(7) Å (Figure 3, right). These substantially divergent bond lengths are a consequence of the ring slippage, moving the center of the Cp ligand away from the metal center and thereby shortening the distance towards the central allylic position. Consequently, the adjacent CF_3 substituent is significantly bent out of plane, with an angle of 24.09(66)°, and the $[C_5(CH_3)_5]^-$ coligand is tiltied out of plane (6.89(50)°), minimizing the steric clash between adjacent CH_3 and CF_3 substituents. Furthermore, the uncoordinated C3−C4 C=C double bond is bent out of plane formed by the allylically bound C5−C1−C2 moiety by an angle of 23.94(56)°. The C1−C2 and C1−C5 bond lengths of 1.482(9) Å and 1.476(9) Å respectively, only differ by 0.006 Å which falls within the error intervals of both bonds, indicating a complete electron delocalization across the allylic system. As a consequence of the allylic structure, the C_{Cp}−C_{Cp} bond length of the unbound positions are significantly shortened and close to those of unconjugated C=C double bonds, at 1.355(10) Å.[20]

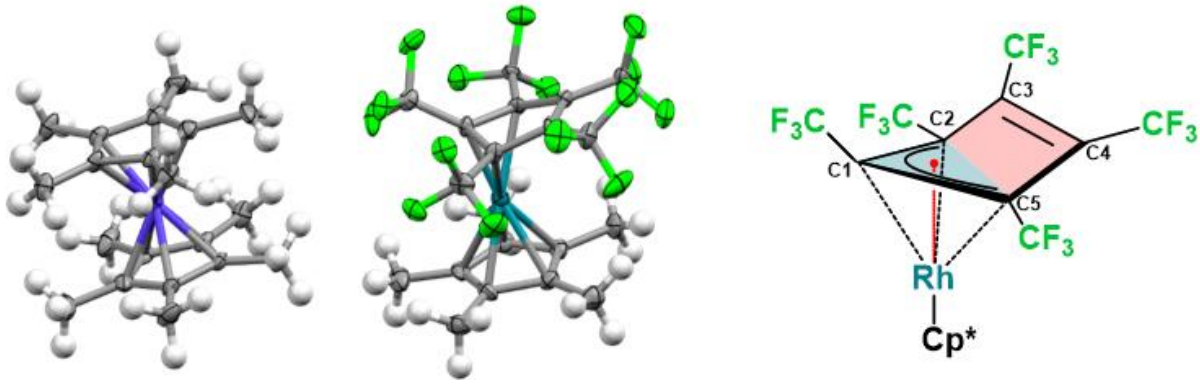

Figure 3. Molecular structure in solid state of $[Co(C_5(CH_3)_5)_2][Rh(C_5(CH_3)_5)(C_5(CF_3)_5]$. Ellipsoids are depicted with 50% probability level. Color code: grey-carbon; green-fluorine; purple-cobalt; turquoise-rhodium (left). Drawing of the allylic bound $[C_5(CF_3)_5]^-$ ligand towards rhodium depicting the C1 bound CF_3 substituent, as well as the unbound C3−C4 double bond tiltied out of plane (right).

We further analyzed the reduction of $[\mathbf{1}]^+$ to $[\mathbf{1}]^-$ quantum chemically by means of energy decomposition analyses (see Table S3 in SI). Adding two electrons to $[1]^+$ populates the e^*_{1g}

orbitals (in D_{5d} notation) of the metallocene. This reduces the π-bonding interaction between ring and metal center by half (lowering $\Delta E_{Orb.Int.}$, see Tables S4 and S3 in SI) and increases Pauli repulsion (ΔE_{Pauli}), leading to a significantly reduced interaction energy (ΔE_{Int}). Slippage of the ring then results in both a symmetry reduction (avoiding near degeneracies in the overall singlet state) and a reduction in Pauli repulsion. At the same time, the orbital interaction is increased significantly. This can be traced back to a strong π back-bonding interaction from the Rh(I) center to the LUMO of the slipped $[C_5(CF_3)_5]^-$ ring (see Table S4 in SI), which is located mostly at the allylic part and is completely absent in $[\mathbf{1}]^+$. The interaction is enhanced by a sizable decrease of the LUMO energy (from −0.59 eV to −2.23 eV) upon distortion. As a result of the structural relaxation, the overall computed interaction energy with the $[C_5(CF_3)_5]^-$ ligand becomes very similar for the Rh(III) and Rh(I) complexes.

Conclusion

The large electron affinity of the $[C_5(CF_3)_5]^-$ ligand and its ability to dramatically shift the redox potential of metallocene anions to less negative values, enabled the first demonstration of a coexistence of metallocene cations $[Co(C_5(CH_3)_5)_2]^+$ and anions $[Rh(C_5(CH_3)_5)(C_5(CF_3)_5)]^-$ $[\mathbf{1}]^-$ in one compound. $[\mathbf{1}]^-$ constitutes the first structurally characterized 4d metallocene anion, further adding to the scarce chemistry of the d block metallocene anions.[21] The reduced interaction energy of $[C_5(CF_3)_5]^-$ towards Rh facilitates η^5/η^3 ring slippage and thereby stabilizes the anionic species by reducing the electron count from 20 to 18 for the Rh(I) center. Hereby, the η^3 structure of the anionic species not only decreases Pauli repulsion but also increases back-bonding interactions, therefore stabilizing the anion in two distinct ways. Compared to the cationic rhodocenium species $[\mathbf{1}]^+$, reduction from Rh(III) to Rh(I) shifts the ^{103}Rh signal from −9308 ppm to −6895 ppm (vs. $Rh(acac)_3$). Quantum chemical calculations have shown that the ^{103}Rh chemical shift of $[\mathbf{1}]^+$ and $[\mathbf{1}]^-$ is largely influenced by the change of geometry, rather than the change in oxidation state.

Authors contribution:

NGK performed synthetic work and performed formal data analysis. MR performed DFT calculations. SSt collected LT-NMR data, R.S. and T.-N. Streit collected and refined XRD data. TNS collected and refined C.V. data. NGK and MR wrote the manuscript. JS collected and simulated the EPR data. NGK, RS, MR, MK and MM revised the manuscript. NGK and MM conceptualized the project. MM coordinated and supervised the project.

Acknowledgements:

Gefördert durch die Deutsche Forschungsgemeinschaft (DFG) –Projektnummer 387284271 – SFB 1349. The authors acknowledge the assistance of the Core Facility BioSupraMol supported by the DFG. R. S. and J. S. thank the Fonds of the Chemical Industry (FCI) for

Kekulé PhD Fellowships. The authors would like to thank the HPC Service of FUB-IT, Freie Universität Berlin, for computing time.

References

[1] a) T. J. Kealy, P. L. Pauson, *Nature* **1951**, *168*, 1039−1040; b) E. O. Fischer, W. Pfab, *Z. Naturforsch. B.* **1952**, *7*, 377−379; c) G. Wilkinson, M. Rosenblum, M. C. Whiting, R. B. Woodward, *J. Am. Chem. Soc.* **1952**, *74*, 2125−2126.

[2] M. Patra, G. Gasser, *Nat. Rev. Chem.* **2017**, *1*, 0066.

[3] S. M. Beladi-Mousavi, S. Sadaf, A.-K. Hennecke, J. Klein, A. M. Mahmood, C. Rüttiger, M. Gallei, F. Fu, E. Fouquet, J. Ruiz, D. Astruc, L. Walder, *Angew. Chem. Int. Ed.* **2021**, *60*, 13554−13558.

[4] B. Verlhac, N. Bachellier, L. Garnier, M. Ormaza, P. Abufager, R. Robles, M.-L. Bocquet, M. Ternes, N. Lorente, L. Limot, *Science* **2019**, *366*, 623−627.

[5] G. G. Hlatky, *Coord. Chem. Rev.* **1999**, *181*, 243−296.

[6] G. Gritzner, J. Kuta, *Pure Appl. Chem.* **1984**, *56*, 461−466.

[7] a) M. G. Walawalkar, P. Pandey, R. Murugavel, *Angew. Chem. Int. Ed.* **2021**, *60*, 12632−12635; b) A. J. Bard, E. Garcia, S. Kukharenko, V. V. Strelets, *Inorg. Chem.* **1993**, *32*, 3528−3531.

[8] J. M. Rall, M. Lapersonne, M. Schorpp, I. Krossing, *Angew. Chem. Int. Ed.* **2023**, *62*, e202312374.

[9] M. Malischewski, M. Adelhardt, J. Sutter, K. Meyer, K. Seppelt, *Science* **2016**, *353*, 678−682.

[10] a) C. Magnoux, D. P. Mills, *Eur. J. of Inorg. Chem.* **2022**, *2022*, e202101063; b) J. C. Smart, J. L. Robbins, *J. Am. Chem. Soc.* **1978**, *100*, 3936−3937; c) M. Malischewski, K. Seppelt, *Dalton Trans.* **2019**, *48*, 17078−17082; d) D. Baudry, M. Ephritikhine, *J. Chem. Soc., Chem. Comm.* **1979**, 895−896; e) B. M. Gardner, J. McMaster, W. Lewis, S. T. Liddle, *Chem. Commun.* **2009**, 2851−2853; f) F. Hung-Low, C. A. Bradley, *Inorg. Chem.* **2013**, *52*, 2446−2457; g) M. Saito, N. Matsunaga, J. Hamada, S. Furukawa, T. Tada, R. H. Herber, *Chem. Lett.* **2018**, *48*, 163−165; h) S. M. Greer, Ö. Üngor, R. J. Beattie, J. L. Kiplinger, B. L. Scott, B. W. Stein, C. A. P. Goodwin, *Chem. Commun.* **2021**, *57*, 595−598; i) C. A. P. Goodwin, M. J. Giansiracusa, S. M. Greer, H. M. Nicholas, P. Evans, M. Vonci, S. Hill, N. F. Chilton, D. P. Mills, *Nat. Chem.* **2021**, *13*, 243−248; j) S. Harder, M. H. Prosenc, *Angew. Chem., Int. Ed. Engl.* **1996**, *35*, 97−99; k) S. Harder, M. H. Prosenc, *Angew. Chem., Int. Ed. Engl.* **1994**, *33*, 1744−1746; l) S. Harder, M. H. Prosenc, U. Rief, *Organometallics* **1996**, *15*, 118−122; m) S. Harder, *Coord. Chem. Rev.* **1998**, *176*, 17−66.

[11] a) N. G. Connelly, W. E. Geiger, *Chem. Rev.* **1996**, *96*, 877−910; b) R. C. Wheland, *J. Am. Chem. Soc,* **1976**, *98*, 3926−3930.

[12] a) K. Sünkel, S. Weigand, A. Hoffmann, S. Blomeyer, C. G. Reuter, Y. V. Vishnevskiy, N. W. Mitzel, *J. Am. Chem. Soc.* **2015**, *137*, 126−129; b) W. Erb, N. Richy, J.-P. Hurvois, P. J. Low, F. Mongin, *Dalton Trans.* **2021**, *50*, 16933−16938.

[13] a) M. Malischewski, R. Sievers, J. Parche, N. G. Kub, *Synlett* **2023**, *34*, 1079−1086; b) P. G. Gassman, C. H. Winter, *J. Am. Chem. Soc.* **1986**, *108*, 4228−4229.

[14] a) E. D. Laganis, D. M. Lemal, *J. Am. Chem. Soc.* **1980**, *102*, 6633−6634; b) R. D. Chambers, S. J. Mullins, A. J. Roche, J. F. S. Vaughan, *J. Chem. Soc., Chem. Commun.* **1995**, 841; cR. D. Chambers, A. J. Roche, J. F. S. Vaughan, *Can. J. Chem.* **1996**, *74*, 1925−1929.

[15] a) M. S. Robin Sievers, Susanne M. Rupf, Joshua Parche, Dr. Moritz Malischewski, *Angew. Chem. Int. Ed.* **2022**, *61*, e202211147; b) J. Parche, S. M. Rupf, R. Sievers, M. Malischewski, *Dalton Trans.* **2023**, *52*, 5496−5502; c) N. G. Kub, R. Sievers, J. Parche, M. Malischewski, *Chem. Eur. J.* **2024**, *30*, e202400427; d) R. Sievers, M. Reimann, N. G. Kub, S. M. Rupf, M. Kaupp, M. Malischewski, *Chem. Sci.* **2024**.

[16] R. Sievers, M. Malischewski, *unpublished results* **2025**.

[17] J. L. Robbins, N. M. Edelstein, S. R. Cooper, J. C. Smart, *J. Am. Chem. Soc.* **1979**, *101*, 3853−3857.
[18] a) M. Jochriem, L. A. Casper, S. Vanicek, D. Petersen, H. Kopacka, K. Wurst, T. Müller, R. F. Winter, B. Bildstein, *Eur. J. Inorg. Chem.* **2020**, *2020*, 1300−1310; b) N. El Murr, J. E. Sheats, W. E. Geiger, Jr., J. D. L. Holloway, *Inorg. Chem.* **1979**, *18*, 1443−1446; c) O. V. Gusev, L. I. Denisovich, M. G. Peterleitner, A. Z. Rubezhov, N. A. Ustynyuk, P. M. Maitlis, *J. Organomet. Chem.* **1993**, *452*, 219−222.
[19] a) V. Hosseininasab, I. M. DiMucci, P. Ghosh, J. A. Bertke, S. Chandrasekharan, C. J. Titus, D. Nordlund, J. H. Freed, K. M. Lancaster, T. H. Warren, *Nat. Chem.* **2022**, *14*, 1265−1269; b) M. M. Clark, W. W. Brennessel, P. L. Holland, *Acta Cryst. E.* **2009**, *65*, m391.
[20] D. R. Lide, *Tetrahedron* **1962**, *17*, 125−134.
[21] Deposition number CCDC 2416649 and 2416650 contain the supplementary crystallographic data for this paper. This data is provided free of charge by the joint Cambridge Crystallographic Data Centre and Fachinformationszentrum Karlsruhe Access Structures service www.ccdc.cam.ac.uk/structures.